JOURNAL OF OPTOELECTRONICS AND ADVANCED MATERIALS, Vol. 11, No. 6, June 2009, p. 880 - 886

Effect of organic modification on oxygen sensing properties of xerogel with a covalently linked ruthenium(II) complex

YANHONG LIU[a,b], BIN LI[a*], XIUDONG WU[c], YAN CONG[a,b]

[a]*Key Laboratory of Excited State Processes, Changchun Institute of Optics, Fine Mechanics and Physics, Chinese Academy of Sciences, Changchun 130033, P. R. China*

[b]*Graduate School of the Chinese Academy of Sciences, Chinese Academy of Sciences, Beijing 100039, P. R. China*

[c]*Faculty of Chemistry, Northeast Normal University, Changchun 130024, PR China*

A series of organic-inorganic hybrid composites were prepared from methyltriethoxylsilane (MTEOS) /tetraethylorthosilane (TEOS) xerogels chemically doped with a Ru(II) complex. The effect of MTEOS/TEOS molar ratio on the luminescence and oxygen sensing properties has been systematically investigated based on the luminescence intensity quenching. Moreover, the effects of MTEOS/TEOS molar ratio on the structure change in the matrix and the bonding between the probes and the matrix were studied by Fourier transform infrared spectroscopy (FTIR) and electronic absorption spectra etc in detail for a better understanding of the oxygen sensing behaviors. The experimental results show blue shift in the emission wavelength of Ru(II) complex entrapped within MTEOS/TEOS compared with that in the pure silica matrix. And the oxygen sensitivity was found to increase with increasing molar ratio of MTEOS to TEOS owing to the decreased polarity of the microenvironment around the Ru(II) molecules. Leaching study was also performed for testing the bonding between the probes and the xerogel matrix, which shows that parts of the indicator dyes would elute from the matrix for the xerogel containing more than 20% MTEOS because of less Si-OH groups with which the dyes could react to form covalent bond.

(Received April 29, 2009; accepted June 15, 2009)

Keywords: Oxygen sensing, Ormosils, Covalent bond, Ru(II) complex

1. Introduction

The determination of oxygen concentrations in both gaseous and aqueous media has long been the focus in many areas of industry control, pollution monitoring, medicine and everyday life. In the past decade, optical oxygen sensors based on luminescence quenching by oxygen on the intensity (I) or excited lifetime (τ) of a luminophore have become more and more attractive compared with conventional amperometric devices owing to the advantages of quick response time, no consumption of oxygen, high sensitivity and high resolution as well as continuous determination of oxygen concentrations in remote, hazardous, or in vivo environments [1,2]. They are composed of an oxygen-sensitive indicator dye dispersed within oxygen permeable matrix [3-5] for practical applications in optical oxygen sensing devices.

Organically modified silicas (ormosils), in which organic fragments are built into silicon-oxide network, have been demonstrated promise in the area of luminescence-based oxygen sensors. It has been found that organically modified precursors could improve the sensor's service life, sensitivity and dynamic range measurement. A number of organic modifiers have been reported, for example methyltriethoxysilane (MTEOS) [6-10], ethyltriethoxysilane (ETEOS) [10,11] and octyltriethoxysilane (OtEOS) [12,13]. However, current ormosil oxygen sensors are mainly based on the physical entrapment of the probes in the matrix. There are still significant drawbacks including leaching of the indicator dyes, and poor flexibleness because only weak physical interactions exist between the dopant and the matrix.

Ruthenium(II) complexes have been used extensively as the indicator dyes for luminescence-based oxygen-sensing applications [14,15] due to their high photochemical stability, high extinction coefficient, relatively long lifetime determined by the metal to ligand charge transfer (MLCT) excited states, large Stokes shift, and absorption spectra that nearly matches the emission spectrum of inexpensive, commercially available blue LED's. Recently, Ru(II) complexes have been successfully grafted to pure silica without significant changes in the photoluminescence (PL) properties but increasing the stability and sensing performances [14,16-18].

Employing the advantages of both ormosil and covalent bonding strategy, a series of ormosil xerogels consisting of a $[Ru(phen)_2(bpy)]^{2+}$ portion covalently bonded to MTEOS/TEOS derived silica matrix were prepared in this work via a simple sol-gel approach. Oxygen sensing properties of the Ru(II)-ormosil (MTEOS/TEOS) were systematically investigated and the performances were discussed based on the luminescence intensity quenching. In addition, the effects of MTEOS/TEOS molar ratio on the structure change in the matrix, and the bonding between the probes and the matrix were studied by FTIR and electronic absorption spectra in detail.

2. Experimental

2.1 Reagents and measurement

Anhydrous $RuCl_3$ (99.99%), 3-aminopropyltriethoxysilane (APS) and MTEOS were obtained from Aldrich (Milwaukee, WI. USA) and used as received. Thionyl chloride ($SOCl_2$, A.R.) was obtained from Shanghai Chemical Company. $SOCl_2$ was used after distillation in vacuo. Tetrathoxysilane (TEOS) and alcohol (EtOH) were purchased from Tianjin Chemicals Company. The complex bis(1,10-phenanthroline) ruthenium(II) chloride dehydrate, $Ru(phen)_2Cl_2.2H_2O$, was synthesized and purified as described in the literature [19]. 4,4′-Dimethyl-2,2′-bipyridyl and 2,2′-bipyridine-4,4′-dicarboxylic acid were prefabricated as the literature [20].

The IR absorption spectra were measured in the region of 400-4500 cm^{-1} by a Fourier transform infrared (FTIR) spectrophotometer (Model Perkin-Elmer Model 580B) with a resolution of ± 4 cm^{-1} using the KBr pellet technique. The absorption spectra of xerogel powders and oxygen sensing properties based on luminescence intensity quenching were characterized using a Hitachi-4500 fluorescence spectrophotometer equipped with a xenon lamp (150 W) operating in the range of 200-900 nm. For the Stern-Volmer plots measurements, oxygen and nitrogen were mixed at different concentrations via gas-flow controllers and flowed directly into the gas chamber sealed with a close fitting suba-seal rubber lid equipped with two (in and out) tubes. 1 min is usually allowed between changes of the N_2/O_2 concentrations to ensure that a new equilibrium point had been established. Equilibrium was evident when the luminescence intensity remained constant (±2%). Sensing response curves were obtained using the same instruments.

In the measurement of fluorescence lifetime of the Ru complex incorporated within the xerogels, a 355 nm light generated from the Third-Harmonic-Generator pumped by a pulsed Nd:YAG laser was used as an excitation source. The Nd:YAG laser was with a line width of 1.0 cm^{-1}, pulse duration of 10 ns and repetition frequency of 10 Hz. The UV–vis electronic absorption measurements of the elution solutions were performed with a Shimadzu UV-3000 spectrophotometer with a resolution of ±1 nm. All measurements were performed at ambient temperature.

2.2 Synthesis

2.2.1 Synthesis of 2,2′-bipyridine functionalized Bpy-Si hydrolysable ligand

The alkoxysilane-modified bipyridine ligand (denoted as Bpy-Si) was prepared using 2,2′-bipyridine 4,4′-dicarboxylic acid and APS as the starting materials according to the literature [17,21]. The detailed synthetic procedure can be briefed as follows: 1.00 mmol 2,2′-bipyridine-4,4′-dicarboxylic acid was dissolved in 4 mL distilled $SOCl_2$ and refluxed for 4 h. Excess $SOCl_2$ was eliminated by evaporation from the yellow solution, and the residual was reacted with APS under nitrogen for 4 h at room temperature in the presence of excess pyridine using 20 mL diethyl ether as a solvent. Pyridinium hydrochloride was filtered and evaporation of the residual organic solvent finally gave the alkoxysilane-modified bipyridine ligand Bpy-Si.

2.2.2 Synthesis of the hydrolysable $Ru(phen)_2(Bpy\text{-}Si)Cl_2$

A mixture of $Ru(phen)_2Cl_2$ and Bpy-Si (molar ratio 1:1.02) in anhydrous ethanol was refluxed for 8 h under nitrogen atmosphere to give a transparent deep red solution. Finally ethanol was rotary evaporated off and the residue was dried in vacuum.

2.2.3 Preparation of Ru(II) covalently bonded ormosil xerogels

The typical xerogel fabrication process is as follows: TEOS was added to the $Ru(phen)_2(Bpy\text{-}Si)Cl_2$ ethanol solution in a plastic vial, followed by addition of H_2O and HCl. The final molar ratio of constituents was $TEOS:H_2O:C_2H_5OH:HCl = 1:4:4:0.01$. The concentration of $Ru(phen)_2(Bpy\text{-}Si)Cl_2$ used here was 1×10^{-4} M with respect to the final sol. The solution was sealed and magnetically stirred at room temperature for 10 h. Then the sol solution was kept in dark under ambient condition for 2 days, and dried at 60°C with loosely capped lids for 2 weeks. Finally optical transparent bulk monolithic xerogel was obtained. The transparent monolithic xerogel was grounded in an agate mortar for further characterizations (denoted as sample Ru-0%). This procedure was chosen because it is representative of xerogels reported in the literatures [9,10,18,22]. The synthetic procedure of MTEOS/TEOS composite xerogels (see the final structure shown in Scheme 1.) was similar to the above-mentioned preparation of TEOS-based xerogel but with mixed TEOS and MTEOS solutions containing 20, 40 and 60 mol% MTEOS, repectively (denoted as sample Ru-20%, Ru-40% and Ru-60%).

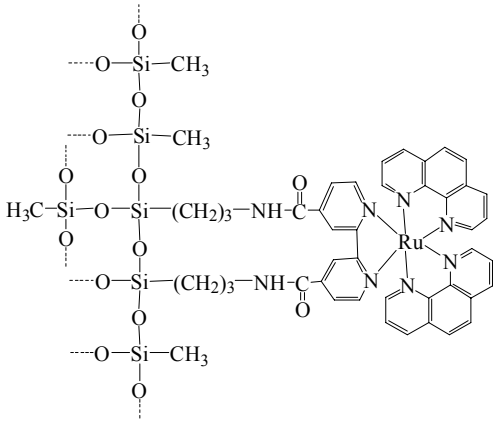

Scheme 1. The typical obtained structure of the final xerogel sample.

3. Results and discussion

3.1 FTIR spectra analysis

The FTIR spectra of all the xerogel samples are shown in Fig. 1. The presence of the Ru(II) complex covalently bonded to the network was supported by FTIR. For Ru/0%, the peak at 1639 cm^{-1}, originating from the –CONH- group of Bpy-Si is observed, which is consistent with the fact that the Bpy-Si group in the framework remains intact after the hydrolysis/condensation reaction [17,23]. The remained ν(Si–C) vibrating absorption located at 1278 cm^{-1} indicates that the Si–CH_2 bond keeps stable during the reactions. For all the samples concerned, there is a very pronounced absorption band appearing at 1047–1074 cm^{-1} (ν_{as}, Si–O), together with two less pronounced bands at 775–798 (ν_s, Si–O) and 420–451 cm^{-1} (δ, Si–O–Si) corresponding to the vibration absorption of Si-O-Si groups (ν represents stretching, δ in-plane bending, s symmetric, and as asymmetric vibrations), indicating the formation of the silica network [24].

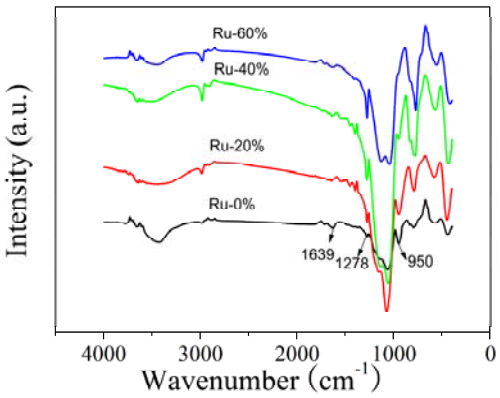

Fig. 1. Representative FTIR spectra from Ru-0% to Ru-60%.

A weak band located at ~950 cm^{-1} is attributed to Si-OH bending vibration, and the wide band between 3100 and 3700 cm^{-1} is attributed to the stretching modes of the residual Si–OH and the adsorbed water. As shown in Fig. 1, the intensity of the Si–OH absorption band decreases with the increasing molar ratio of MTEOS to TEOS. The band at 1278 cm^{-1} is assigned to the symmetric deformation modes of -CH_3 [25,26]. The enhancement of the -CH_3 vibration peaks, with the increasing molar ratio of MTEOS to TEOS, indicates that the three-alkyloxyl-functionalized silane precursor (MTEOS) could homo-polymerize or co-polymerize with the four-alkyloxyl -functionalized silane precursor (TEOS) to form silica networks.

3.2 Spectroscopic analysis

Fig. 2 represents the electronic absorption spectra. All the xerogel samples show an intense absorption band observed at about 475 nm, which can be assigned to the MLCT ($t_{2g}(Ru)\rightarrow\pi^*(L)$) transition [17]. As shown in Fig. 2, no absorption band shift was observed for the Ru(II) complex, regardless of the matrix employed. Fig. 3 shows the emission spectra of the samples with excitation at 470nm, in which blue shifts of the emission wavelength were observed from Ru-0% to Ru-60%. This indicates that the microenvironment around the Ru(II) molecules affects only the extent of relaxation from the MLCT excited state without perturbing the Franck-Condon excited state level. The blue shifts can be explained as follows: For Ru/0%, the residual solvents and Si–OH groups in the matrix can stabilize the MLCT excited state to lower energy level due to the dipole-dipole interaction [27]. However, the residual Si–OH groups decrease with increasing MTEOS content due to replacement by -CH_3, which has been observed in the FTIR spectra. So the excited state can not be completely stabilized within its lifetime and the emission is from relaxation of higher-energy unequilibrated state, which leads to the blue-shift in the emission spectra.

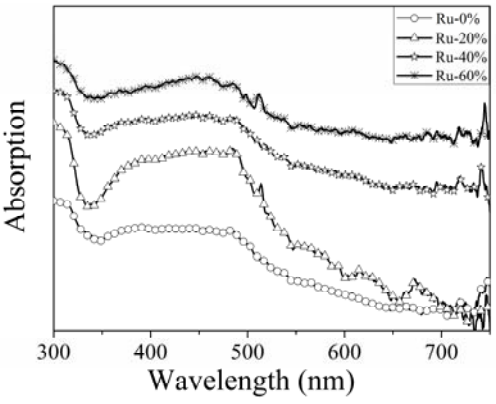

Fig. 2. Electronic absorption spectra from Ru-0% to Ru-60%.

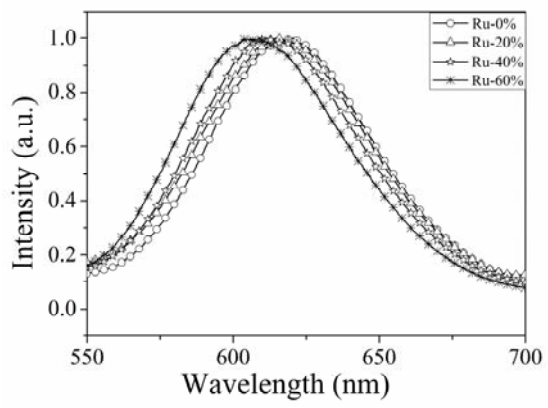

Fig. 3. Room temperature emission spectra at λ_{ex} = 470 nm.

3.3 Oxygen sensing properties analysis

Fig. 4 shows the luminescence intensity Stern-Volmer plots for all the samples from Ru-0% to Ru-60%. The sensitivity I_0/I_{100} was increased from 4.3 to 6.0, which was consistent with reported ormosils in the literature [12]. The observed improvement in sensitivity is attributed to the decreased polarity provided by the nonhydrolyzing Si-CH_3 functional group. Since MTEOS contains three hydrolyzable alkoxy groups, the Si-CH_3 bonds remain intact under sol-gel synthesis conditions, being part of the three dimensional silica backbone after gel formation and structurally act as network modifiers that terminate the silica network. So sol-gels formed from MTEOS provide a more hydrophobic environment that is favorable for oxygen sensors. It has also been reported previously that the Ru(II) complex showed improved luminescence quenching by oxygen when immobilized in materials of increased nonpolarity [28-30].

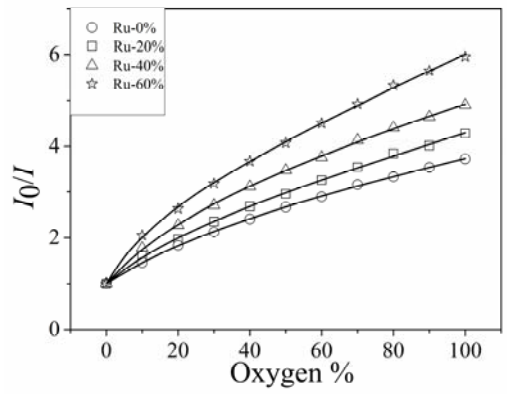

Fig. 4. Typical Stern–Volmer plot of the xerogel samples. The solid lines represent the fit using Demas two site model using eq.3.

For well behaved oxygen-sensing materials in which the luminophore is dispersed uniformly within homogeneous media, the intensity I or lifetime τ of the luminophore fits the linear Stern-Volmer equation [16,31]

$$I_0/I = \tau_0/\tau = 1+K_{sv}pO_2 = 1+K_q\tau_0\, pO_2 \quad (1)$$

where pO_2 is the partial pressure of oxygen at 1 atmosphere pressure, τ_0 and τ are lifetimes, I_0 and I are intensities. The subscript 0 denotes the absence of quencher. K_{sv} is the Stern-Volmer constant. K_q is the bimolecular quenching constant. A plot of I_0/I or τ_0/τ versus oxygen concentration should give a linear relationship with a slope of K_{SV}, and an intercept of 1 on the y-axis. The lifetime decay of luminophore in homogeneous media can be described by a single exponential equation [30,32]

$$I(t) = \alpha\exp(-t/\tau) \quad (2)$$

where $I(t)$ is the luminescence intensity at time t, and α is the preexponential factor. However, the plots deviate from linearity especially at low oxygen concentration as shown in Fig. 4. The Stern-Volmer equation is usually nonlinear when quenching takes place in a solid matrix. Two mechanism models were used to explain this: (1) Demas two-site model ascribes it to that the complex exists in two distinctly different environments, with both being quenchable but with different quenching sensitivity; (2) Lehrer model ascribes it to that the complex exists in two distinctly different environments, with one being quenchable and the other being unquenchable.

In Demas two-site model, the linear Stern-Volmer equation [5,14] then becomes

$$\frac{I_0}{I} = \frac{1}{f_{01}/(1+K_{sv1}P_{O_2}) + f_{02}/(1+K_{sv2}P_{O_2})} \quad (3)$$

where f_{0i} values are the fraction of each of the two sites contributing to the unquenched intensity, pO_2 is the partial pressure of oxygen at 1 atmosphere pressure, and K_{SVi} values are the associated Stern-Volmer quenching constants for the two sites. Meanwhile, when K_{SV2} = 0, the Demas model collapses to Lehrer model [16,33], which is also able to fit the experiment data reasonably. The equation is shown below:

$$\frac{I_0}{I} = \frac{1}{f_{01}/(1+K_{sv1}pO_2) + (1-f_{01})} \quad (4)$$

At low oxygen concentration, easily accessible luminescence molecules are quenched more effectively, whereas the less accessible domains are increasingly dominating when the quenching occurs at high oxygen concentrations.

Both Demas two-site model and Lehrer model were used to fit the intensity-quenching curves of all the samples. The fitting parameters are given in Table 1. Demas model fits better to the experimental data. As

shown in Fig. 4, the solid lines represent the best-fitting plots using Demas two sites model. The fitting parameters summarized in Table 1 show that the Stern-Volmer constant associated with the more readily quenched site, K_{SV1}, are ~15-fold more sensitive to O_2 than K_{SV2} that associated with the less readily quenched site.

Table 1. Intensity-based Stern-volmer oxygen quenching parameters from the fitting employing different models, that is, Demas Two-site model and Lehrer Model.

	Demas Model				Lehrer Model		
	f_{01}	$K_{sv1}(O_2\%^{-1})$	$K_{sv2}(O_2\%^{-1})$	r^2	f_{01}	$K_{sv1}(O_2\%^{-1})$	r^2
Ru-0%	**0.7155**	**0.0907**	**0.0076**	**0.9994**	**0.8723**	**0.0510**	**0.9992**
Ru-20%	**0.7557**	**0.0663**	**0.0045**	**0.9998**	**0.8927**	**0.0590**	**0.9983**
Ru-40%	**0.7858**	**0.1106**	**0.0055**	**0.9996**	**0.8929**	**0.0803**	**0.9985**
Ru-60%	**0.7494**	**0.1773**	**0.0098**	**0.9995**	**0.9135**	**0.0994**	**0.9966**

In the Demas two-site model, there are two excited-state lifetime components for the luminescence species, and the excited lifetime decay may be described by [16]

$$I(t) = \alpha_1 \exp(-t/\tau_1) + \alpha_2 \exp(-t/\tau_2) \quad (5)$$

where $I(t)$ represents the fluorescence intensity at time τ, the subscripts 1 and 2 denote the assigned lifetime components, and α_i denotes the pre-exponential factors. The weighted mean lifetime τ_M can be calculated by the following equation [32]:

$$\tau_M = \sum_{i=1}^{2} \alpha_i \tau_i \Big/ \sum_{i=1}^{2} \alpha_i \quad (6)$$

The unquenched lifetimes of all the samples under N_2 atmosphere were measured as given in Table 2. The double exponential in eq. 5 provides excellent fits to the experimental data, which further confirms that the Ru(II) molecules occupy the heterogeneous local microenvironment in the matrix.

Table 2. Excited-state lifetime curves decay constants and the response time for the xerogel samples.

	α_1	$\tau_1(\mu s)$	α_2	$\tau_2(\mu s)$	$\tau_M(\mu s)$	r^2	$t_1(s)$	$t_1(s)$
Ru/0%	**0.017**	**0.17**	**0.042**	**1.56**	**1.36**	**0.9972**	**13**	**5**
Ru/20%	**0.022**	**0.17**	**0.060**	**1.80**	**1.6**	**0.9967**	**12**	**7**
Ru/40%	**0.022**	**0.28**	**0.066**	**1.99**	**1.69**	**0.9980**	**13**	**5**
Ru/60%	**0.072**	**2.05**	**0.028**	**0.21**	**1.75**	**0.9981**	**13**	**6**

It has been reported that indicator leakage is one of the main drawbacks of the physical entrapment method. The dye covalently bonded with the matrix can prevent dye leaching from the matrix. Leaching experiments are essential to assess the degree of the dye bonding to the matrix [34]. The xerogel samples were exhaustively extracted in a Soxhlet extractor for a week with 150 mL of alcohol. No detectable leakage by eyes of Ru(II) complexes was observed for Ru-0% and Ru-20%. But for Ru-40% and Ru-60%, the deepening of a yellow color in the extraction was observed, indicating partial leaching of the Ru(II) molecules. Electronic absorption spectra performed on the aliquot solution help to visualize trends in the leaching of the samples. No absorption was detected for Ru-0% and Ru-20%, and the absorption spectra for Ru-40% and Ru-60% are presented in Fig. 5. The investigation revealed that Ru(II) molecules were gradually eluted from the matrix for Ru-40% and Ru-60%. The amount of dyes leached from Ru-40% is substantially less than that leached from Ru-60%. The specific reason for this is still unclear and may be ascribed to the decrease of the reactive sites (Si-OH) of the matrix with increasing methyl incorporation. It can be explained that with increasing methyl incorporation, part of the probes had not been covalently bonded, but adsorbed on the surface of the gel pores and thus could be easily eluted. However, no absorption was observed after additional several days of exposure to alcohol, suggesting that the remaining Ru(II) complex is firmly covalently grafted to the matrix.

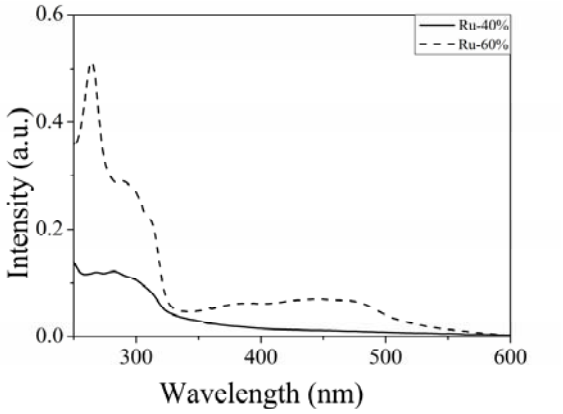

Fig. 5. Absorption spectra of the eluent solution for Ru-40% and Ru-60%.

As an important parameter for oxygen sensors, the reversibility of the previously reported Ru(II)-based sol-gel sensors in the gas phase has also been observed for the samples [14,35]. Fig. 6 represents the typical dynamic response of Ru-20% on exposure to pure N_2 and O_2 atmosphere varied periodically. From the time dependent measurements, the 95% response time ($t_{\downarrow}$) and 95% recovery time ($t_{\uparrow}$) to an alternating atmosphere of pure N_2 and O_2 can also be calculated. Generally, the values are defined as the time taken for a sample to attain 95% of its total emission intensity change when the gas is changed from pure N_2 to pure O_2 ($t_{\downarrow}$) and from pure O_2 to pure N_2 ($t_{\uparrow}$), respectively. The values for all the samples are listed in Table 2. These response times are comparable to those of the sol-gel derived oxygen sensors presented in the literature and such short response times are obviously due to the micropores in the sol-gel matrix [36]. The results also show that the response time is shorter than the recovery time distinctly and this can be explained by the stronger adsorption of oxygen than that of nitrogen on the silica surface [37,38].

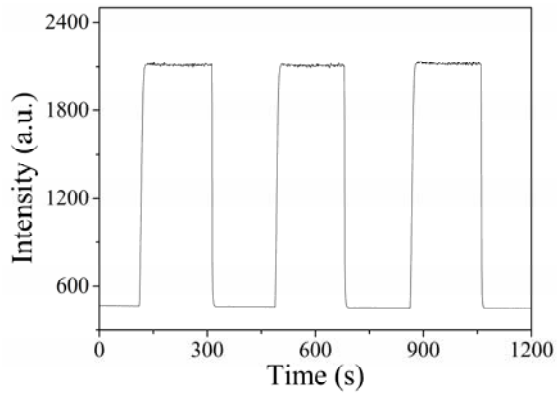

Fig. 6. The typical relative luminescence intensity changes for Ru-20% as a function of time on periodically cycling from 100% nitrogen to 100% oxygen atmosphere.

4. Conclusions

Ru(II) complex was covalently bonded to the MTEOS/TEOS derived xerogels for oxygen sensing via the sol-gel method. The oxygen sensitivity was affected significantly by the increase of the molar percentage of MTEOS within the composites. The sensors presented here exhibit a fast and reversible response to gaseous oxygen. Leaching experiments reveal that part of the indicator dyes elute from the matrix owing to lower number of surface Si-OH groups with increasing methyl incorporation. Our results suggest that it should be possible to covalently graft the Ru(II) complex onto the backbone of ormosils via the co-condensation reaction. This type of ormosil xerogel chemically doped with the indicator dye discussed in this work also appears to provide a viable avenue to improve the performance of sol-gel-derived sensors in dissolved oxygen sensing measurement. The oxygen sensing properties of this kind of covalently grafted functionalized ormosil materials may be further improved via changing the sensor matrix, and continued work is still in progress.

Acknowledgment

The authors gratefully thank the financial supports of the National Natural Science Foundations of China (Grant No. 20571071, 50872130).

Reference

[1] X. Chen, Z. Zhong, Z. Lia, Y. Jiang, X. Wang, K. Wong, Sens. Actuators. B Chem. **87**, 233 (2002).
[2] C. Huo, H. Zhang, B. Yang, P. Zhang, Y. Wang, Inorg. Chem. **45**, 4735 (2006).
[3] Z. Wang, A. R. McWilliams, C. E. B. Evans, X. Lu, S. Chung, M. A. Winnik, I. Manners, Adv. Funct. Mater. **12**, 415 (2002).
[4] S. Anastasova, M. Milanova, E. Kashchieva, H. Funakubo, T. Kamo, N. Grozev, P. Stefanov, D. Todorovsky, Appl. Surf. Sci. **254**, 1545 (2008).
[5] B. W. K. Chu, V. W. W. Yam Langmiur **22**, 7437 (2006).
[6] S. Anastasovaa, M. Milanovaa, S. Rangelovb, D. Todorovskya, J. Non-Cryst. Solids **354**, 4909 (2008).
[7] J. B. Bharathibai, Sens. Actuators. B Chem. **123**, 568 (2007).
[8] C. M. McDonagh, F Sheridan, T Butler, B. D. MacCraith, J. Non-Cryst. Solids **194**, 72 (1996).
[9] C. M. McDonagh, P Lowe, K Mongey, B. D. MacCraith, J. Non-Cryst. Solids **306**, 138 (2002).
[10] C. M. McDonagh, B. D. MacCraith, A. K. McEvoy, Anal. Chem. **70**, 45 (1998).
[11] P. Lavin, C. M. McDonagh, B. D. MacCraith, J. Sol-Gel Sci. Tech. **13**, 641 (1998).
[12] Y. Tang, E. C. Tehan, Z. Tao, F. V. Bright, Anal. Chem. **75**, 2407 (2003).
[13] A. N. Murashkevich, V. G. Vashina, I. M. Zharskii, J . Sol-Gel Sci. Tech. **20**, 7 (2001).
[14] B. Lei, B. Li, H. Zhang, S. Lu, Z. Zheng, W. Li, Y. Wang, Adv. Funct. Mater. **16**, 1883 (2006).
[15] R. M. Bukowski, R. Ciriminna, M. Pagliaro, F. V. Bright, Anal. Chem. **77**, 2670 (2005).
[16] B. F. Lei, B. Li, H. Zhang, L. Zhang, W. Li, J. Phys. Chem. C **111**, 11291 (2007).
[17] Zhang HR, Li B, Lei BF, Li WL, Lu SZ (2007) Sens Actuators B Chem 123: 508.
[18] X. D. Wu, Y Cong, Y. H. Liu, J. Sol-Gel Sci. Tech. **49**, 355 (2009).

[19] B. P. Sullivan, D. J. Salmon, T. J. Meyer, Inorg. Chem. **78**, 3334 (1978).
[20] G. Sprintschnik, H. W. Sprintschnik, P. P. Kirsch, D. G. Whitten J. Am. Chem. Soc. **99**, 4947 (1977).
[21] H. R. Li, J Lin, H. J. Zhang, H. C. Li, L. S. Fu, Q. G. Meng, Chem. Commun. 1212 (2001).
[22] C. Malins, S. Fanni, H. G. Glever, J. G. Vos, B. D. MacCraith, Anal. Commun. **36**, 3459 (1999).
[23] J. L. Liu, S Xu, B Yan J. Optoelectron. Adv. Mater. **10**, 3357 (2008).
[24] H. Zhu, Y. G. Ma, Y. G. Fan, J. C. Shen, Thin Solid Films **397**, 95 (2001).
[25] X. C. Li, A. K. Terence, J. Non-Cryst. Solids **204**, 235 (1996).
[26] P. Innocenzi, M. O. Abdirashid, M. Gugielmi, J. Sol-gel Sci. Tech. **3**, 45 (1994).
[27] G. D. Qian, Z. Yang, C. L.Yang, J. Appl. Phys. **88**: 2503 (2000).
[28] W. Y. Xu, R. C. McDonagh, B. Langsdorf, J. N. Demas, B. A. DeGraff Anal. Chem. **66**, 4133 (1994).
[29] M. T. Murtagh, H. C. Kwon, M. R. Shahriari, M. Krihak, D. E. Ackley, J. Mater. Res. **13**, 3326 (1998).
[30] Z. Y.Tao, C. T. Elizabeth, Tang Y, V. B. Frank, Anal. Chem. **78**, 1939 (2006).
[31] V. O. Stern, M. P. Volmer Zeitschr **20**, 183 (1919).
[32] M. T. Murtagh, M. R. Shahriari, M. Krihak, Chem Mater **10**, 3862 (1998).
[33] S. S. Lehrer Biochemistry **10**, 3254 (1970).
[34] T. Suratwala, Z. Gardlund, K. Davidson, D. R.Uhlmann, J. Watson, S. Bonilla, N. Peyghambarian Chem. Mater. **10**, 199 (1998).
[35] C. S. Chu, Y. L. Lo, Sens. Actuators. B Chem. **124**, 376 (2007).
[36] A. N. Watkins, B. R. Wenner, J. D. Jordan, W. Y. Xu, J. N. Demas, F. V. Bright, Appl. Spectrosc. **52**, 750 (1998).
[37] A. Yekta, Z. Masoumi, M. A.Winnik, Can. J. Chem. **73**, 202 (1995).
[38] H. D. Zhang, Y. H. Sun, K. Q. Ye, P. Zhang, Y. Wang, J. Mater. Chem. **15**, 3181 (2005).

*Corresponding author: lib020@ciomp.ac.cn